

Source Plasma Formation of Field Reversed Configuration for a Long Pulse Operation

TAKAHASHI Tsutomu*, IWATA Kaoru and NOGI Yasuyuki
College of Science and Technology, Nihon University
1-8 Kanda Surugadai, Chiyoda-ku, Tokyo 101-8308, Japan

(Received: 18 January 2000 / Accepted: 1 May 2000)

Abstract

The poloidal flux of a field reversed configuration (FRC) needs to increase more than the present experimental regime to inject a neutral beam into a tangential direction for the plasma heating. Since the poloidal flux of the rigid rotor profile model is proportional to the cube of the separatrix radius, the FRC plasma with a large separatrix radius is produced by the enhancement of the axial contraction. The enhancement is induced by a mirror ratio and a magnetic field index of the compression field. The plasma radius of 1.3 times larger and a poloidal flux of 2.2 times larger than the present experiment status are obtained by high mirror ratio of 1.8 and high magnetic field index of 0.3. The field index is possible to contribute to the adjustment of a radial implosion strength and an axial contraction one and to the control of the ratio of an ion temperature and an electron temperature.

Keywords:

field reversed configuration (FRC), radial compression, axial contraction, mirror ratio, magnetic field index, ratio of ion to electron temperature

1. Introduction

There are several proposals for a long pulse operation of a field reversed configuration (FRC) [1-6]. In the proposals, the plasma of the FRC is heated by a neutral beam injection (NBI) [1-4], an OH transformer [4,5] or a rotating magnetic field (RMF) [6]. The FRC plasma parameters, required for a tangential injection of a deuterium neutral beam with the energy of 10 keV on FIX experiment [2], are as follows. An electron density (n_e) is $\sim 1.0 \times 10^{20} \text{ m}^{-3}$, a normalized separatrix radius (a ratio of a separatrix radius (r_s) and a coil radius (r_w)) $X_s = \sim 0.6$, a poloidal flux $\phi_p = \sim 3.0 \text{ mWb}$, an ion temperature $T_i = 300 \text{ eV}$, an electron temperature $T_e = 100 \text{ eV}$ and the s-number of injection ion $s = 2$.

The plasma parameters except the poloidal flux, are attained by the translation [6] and the usual pinch technique [7]. The poloidal flux of $\sim 3 \text{ mWb}$, under the

compression field of 0.5 T and a coil radius of 0.17 m, requires the normalized plasma radius more than 0.65 on basis of the rigid rotor model [8]. The FRC plasma is also needed to be formed in several times larger bias magnetic field than the present experiment.

In this paper, we propose the FRC plasma formation method with the large X_s and ϕ_p by an adjustment of the radial compression and the axial contraction. The adjustment is controlled by the mirror ratio (R_M) and the magnetic field index of the confinement field ($n_z = z \partial B_z / B_z \partial z$). Preliminary experimental results is presented in the following sections

2. Experimental Apparatus

The theta pinch coil of NUCTE III device is modified. Stepped theta pinch coil elements with 36, 34,

*Corresponding author's e-mail: tom@pyxis.phys.cst.nihon-u.ac.jp

Table 1 Coil Configuration and Plasma Parameter

Case	R_M	\bar{n}_e	τ_{ax}	\bar{v}_{ax}	$\Delta\phi_s$	τ_{Max}	τ_{eq}	$r_s(0)$	l_s	$\tau_{I/e}$	$\tau_{n=2}$
	(cm)	(10^{21})	(μ s)	(cm/ μ s)	(mWb)	(μ s)	(μ s)	(cm)	(cm)	(μ s)	(μ s)
1	1.10	0.03	6.5	3.8	0.15	12.5	30	6.2	62	65	28
2	1.35	0.16	5.0	4.5	0.17	11.0	22	6.5	49	65	28
3	1.38	0.15	4.5	5.5	0.25	8.5	15	6.8	45	60	25
4	1.80	0.24	3.5	6.0	0.2	7.5	15	6.9	60	60	25
5	1.80	0.28	3.0	8.5	0.4	7.0	12	7.8	39	50	22
6	1.80	0.30	3.0	8.5	0.4	7.0	12	8.0	38	50	22

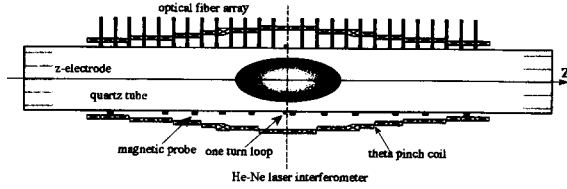


Fig. 1 Schematic overview of the experimental set up on NUCTE-III

32, 30, 28, 26 cm diameter are arrayed symmetrically to the midplane, shown in Fig.1. An averaged decay index ($\bar{n}_z = \int_{-L_c/2}^{L_c/2} n_z dz / L_c$, $L_c \approx 1.35$ m: length between the mirror points) and R_M of the present experiments are listed in Table 1. The theta pinch coil is connected with a 5 kV-1920 μ F slow bank and a 32 kV-67.5 μ F fast one. The bias field has the maximum strength of 0.09 T and the rise time of 90 μ s and the compression field has those of 0.6 T and 4 μ s. A transparent quartz discharge tube with a length of 2.0 m and an inner diameter of about 0.23 m is evacuated till 1.5×10^{-4} Pa and is filled with deuterium gas of 1.33 Pa. A pre-heating plasma is formed by a ringing I_z -discharge method.

An excluded flux array, a single path side-on He-Ne interferometer and an visible fiber array are used to observe the plasma. The sensitivity of the optical array is limited to 550 ± 50 nm by band pass filters [9]. It is confirmed that a dominant component of plasma radiation $I_{br}(z)$ is bremsstrahlung in this region. From a profile of the excluded flux ($\Delta\phi$), a time history of the separatrix radius profile $r_s(z)$ is obtained. An averaged electron density at the midplane ($\bar{n}_e = \int n_e dl / 2r_s(0)$) is calculated from the interferometer. The electron temperature (T_e) is estimated by the following equation,

$$I_{br}(0) \propto \frac{Z_{eff} n_e^2(0)}{\sqrt{T_e}} \quad (1)$$

The value of Z_{eff} is effective charge number. The total plasma temperature (the sum of the electron (T_e) and ion

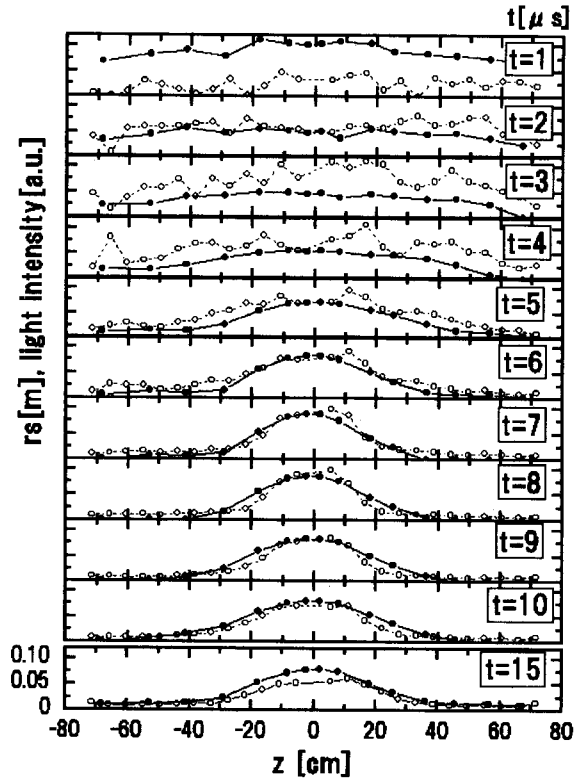


Fig. 2 Time evolution of profiles of a separatrix radius and an intensity of bremsstrahlung in case 6

temperature (T_i), $T_t = T_i + T_e$) is estimated from the equation of the average beta value $\langle \beta \rangle = 1 - x_s^2 / 2$.

3. Experimental Results

The FRC plasma is produced on the six configurations of the theta pinch coil listed in Table 1. The FRC plasmas which have the same $\bar{n}_e \approx 2.2 \times 10^{21}$ m^{-3} and $T_e \approx 120$ eV are compared to clarify the relation between the axial dynamics and the plasma behavior. The time history of $r_s(z)$ and $I_{br}(z)$ of case 6 are shown by closed and open circles, respectively, in Fig.2. The plasma implodes to the center axis by the radial compression. The radial velocity is faster in the coil end region than that in the center one. At 3 μ s, the magnetic reconnection between the bias field and the compression field has been already completed. Then the axial contraction has started from the end region. The hump of $I_{br}(z)$, which indicates the axial contraction, appears at $z = 44$ cm. The front of the contraction arrives to the midplane at 6 μ s. The plasma reaches the equilibrium state at 10 μ s. The value of $r_s(0)$ and separatrix length (l_s) are about 8 cm and 40 cm, respectively.

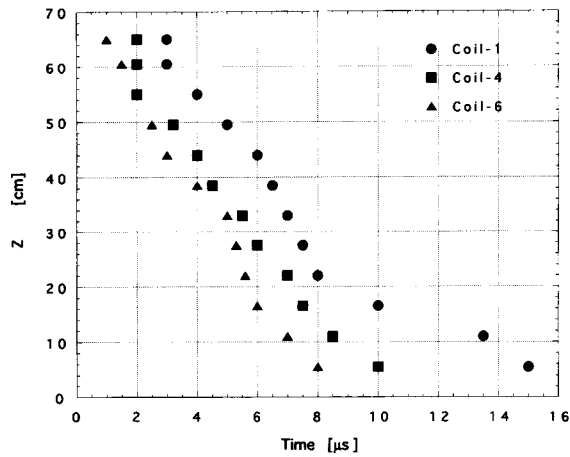


Fig. 3 Time history of front positions of an axial contraction in case 1, case 4 and case 6

On the other hand, in case 1, the radial compression is occurred uniformly over the full length of the coil. The radial velocity is faster than that of case-6 except in the coil end. The hump is formed at 5 μs in the coil end and the axial contraction starts at 7 μs . The front of the hump arrives to the midplane at 15 μs . The equilibrium state is delayed to 25 μs . The separatrix radius and length is about 6 cm and 60 cm.

Figure of 3 shows the position of the front of the hump in cases 1, 4 and 6. Each front travels to $z = 30$ cm with the same velocity of ~ 0.1 m/ μs in the three cases. After that, the front arrives at the midplane with the same velocity in case 6. But with decrease of R_M and \bar{n}_z the velocity is damped and the arrival time is delayed.

In Table 1, the parameters of the axial dynamics, such as the average velocity (\bar{V}_{ax}) from $z = 30$ cm to midplane, the strength of the axial contraction at midplane ($\Delta\phi_s$), onset time (T_{ax}), the arrival time at midplane (T_{Max}) and etc., are summarized at every coils. The value of $\Delta\phi_s$ is calculated from the equation of $\Delta\phi_s = \Delta\phi_p - \Delta\phi_{eq}$ ($\Delta\phi_p$: $\Delta\phi$ at the peak contraction and $\Delta\phi_{eq}$: at the equilibrium state) [10]. The early onset time carries the strong contraction. The maximum of the contraction velocity is about 0.1 m/ μs at $\bar{n}_z = 0.30$ and $R_M = 1.80$.

With increase of \bar{n}_z and R_M , the FRC plasma reaches the equilibrium phase at earlier time and has a larger separatrix radius and a shorter length. The formed plasma has a elliptical shape. The onset time of the $n=2$ instability ($\tau_{n=2}$) is earlier with increase of \bar{n}_z . The life time of the plasma (τ_{life}) is limited by the growth of the instability.

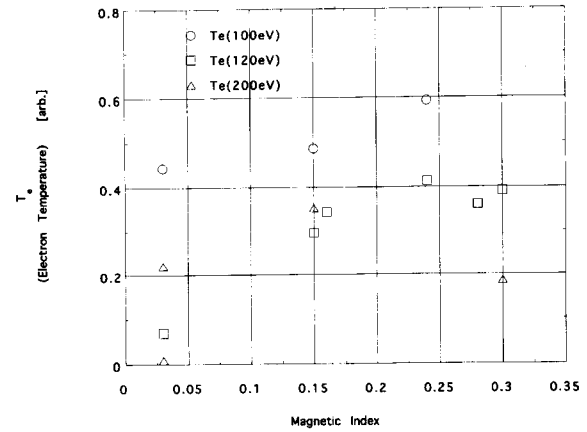


Fig. 4 Relation between an electron temperature and a magnetic field index

The Figure 4 shows the dependence of the electron temperature on the magnetic field index \bar{n}_z . The contribution of Z_{eff} to I_{br} is consider as the same level because of the same T_i and \bar{n}_e . Open triangles, circles and squares show the dependence at the plasma temperature of 195 ± 15 , 120 ± 10 , 100 ± 10 eV. The electron temperature increases with the index of \bar{n}_z .

4. Discussion and Summary

The FRC having a large separatrix radius is produced by the enhancement of the axial contraction that induced by a using a compression field with a high mirror field ratio and/or a large axial magnetic index. Typical value of the separatrix radius at $R_M = 1.8$ and $\bar{n}_z = 0.30$ is $r_s(0) = 8.0$ cm which corresponds to 1.3 times $r_s(0)$ at $R_M = 1.1$ and $\bar{n}_z = 0.03$. Since the poloidal flux in the separatrix surface is proportional to $r_s^3(0)$ on the basis of the rigid rotor profile model [8], 1.3 times $r_s(0)$ means a 2.2 times increase of the poloidal flux. That is, it reaches 1.1 mWb at the former case.

The radial implosion and axial contraction are occurred at the formation phase. The former shock heats ions strongly and the latter heats both ion and electron adiabatically [11,12]. If the former is stronger than the latter, the electron temperature becomes low comparing to the ion one. The present experiment shows that the strong implosion is formed before axial contraction over the full length of the case 1 at $\bar{n}_z = 0.03$. The \bar{n}_z dependence of the electron temperature seen in Fig.4 can be roughly explained from the heating steps.

Further studies will be pursued to produced a target plasma for the neutral beam heating

References

- [1] H. Momota *et al.*, Fusion Technol. **21**, 2307 (1992).
- [2] S. Goto, Y. Yano, S. Sugimoto, Y. Ueda, Y. Ito, S. Ohi and T. Ishimura, Proc. of 10th US-Japan Workshop on Compact Toroids, 71 (1988).
- [3] T. Asai *et al.*, in this conference PI-3.
- [4] H. Ji, M. Yamada, E. Belova, R. Kulsrud, S. Jardin, D. Mikkelsen and S. Zweben, Bull. Am. Phys. Soc. **44**, 45 (1999).
- [5] T. Matsuyama, L. Yongwan, Y. Ono and M. Katsurai, Bull. Am. Phys. Soc. **44**, 44 (1999).
- [6] J.T. Slough and A. L. Hoffman, Bull. Am. Phys. Soc. **44**, 42 (1999).
- [7] Y. Ookuma, M. Urano, M. Narushima, T. Takahashi and Y. Nogi, Nucl. Fusion **38**, 1501 (1998).
- [8] W.T. Armstrong, R.K. Linford, J. Lipson, D.A. Platts and E.G. Shorwood, Phys. Fluids **24**, 2068 (1981).
- [9] T. Takahashi, T. Assai, Y. Narushima, Y. Ohkuma and Y. Nogi, Proc. of 1st APAF & 3rd APPTC98, 92 (2000).
- [10] R.D. Milroy and J.T. Slough, Phys. Fluids **30**, 3566 (1988).
- [11] M. Tuszewski, Phys. Fluids **31**, 3754 (1988).
- [12] J.K. Wright, R.D. Medford and B. Chambers, Proc. 5th Intern. Conf. Ionization Phenomena in Gases, 2147 (1961).